Manuscript ID: 298519
DOI:10.18462/iir.iccc.2020.298519

Influence of microwave assisted freezing parameters on ice crystal growth

Graziele GUSTINELLI[(a)], Patricia ANDREU-CABEDO[(b)], Estefania LOPEZ-QUIROGA[(b)], Epameinondas XANTHAKIS[(a)]

[(a)] RISE-Agrifood and Bioscience
Gothenburg, 41276, Sweden, epameinondas.xanthakis@ri.se
[(b)] School of Chemical Engineering, University of Birmingham
Birmingham, B15 2TT, United Kingdom, E.Lopez-Quiroga@bham.ac.uk

ABSTRACT

Final quality of frozen foods is determined by the shape and size of the formed ice crystals, as they might cause irreversible damage to the cellular structure –crystals larger than cells will break them appart, impairing quality. Recent studies using microwave assisted freezing (MAF) – a novel alternative freezing technology – have shown that microwave radiation can influence the ice crystal formation leading to crystal size reduction. Two concepts have been proposed regarding the mechanism of action such as "NITOM" concept (Nucleation Induced by Temperature Oscillation caused by MWs) and the "NIMIW" (Nucleation Induced by constant or pulsed MIcroWaves power). The present study aimed to enlighten the influence of different microwave assisted freezing parameters on the ice crystal growth. A Response Surface Method (RSM) has been used to evaluate the effect of three process parameters (i.e. MW pulse width, power and cooling rate) on final crystal size, correlating processing conditions to final crystal sizes and setting the basis for further analysis.

Keywords: Microwave Assisted Freezing, Food, Novel technologies

1. INTRODUCTION

Freeze damage in cellular matrices is a major challenge in the Food Industry. Freezing of food matrices is ruled by water crystallisation. Thus, final quality of frozen products depends on the phase transition from water into ice. The size of the ice crystals is critical for the final quality of the frozen food as it can cause irreversible damage to the cellular structure, which in turn degrades the texture and color of the product. For this reason, several emerging technologies are focusing on controlling the crystallization process, i.e. controlling the rate of ice crystal formation and growth. Most of these technologies take advantage of the physical properties and the characteristics of the water molecules.

Water molecules react when electric or magnetic fields try to disturb its equilibrium state (Dalvi-Isfahan et al., 2016; Jha et al., 2017a). Electrical and magnetic disturbances are factors that could rearrange the hydrogen-bonded network of water. Recent studies on the application of external static electric fields to freezing of real food systems (Xanthakis et al., 2013; Le-Bail et al., 2016; Dalvi-Isfahan et al., 2017; Jha et al., 2017b) showed freezing in the presence of high voltage static electric field (electro-freezing) significantly reduced the damage to food microstructure, improving the quality of the frozen product.

Concerning the electromagnetic effects on water, Chaplin (2013) reported that the presence of electromagnetic fields (EMF) leads to a reorientation the water molecules, and some hydrogen bonds of the network may be broken. Electric fields are more efficient in changing the conformation of water network due to the intrinsic electric dipole moment of water molecule, while much stronger magnetic fields are required in order to exert the same force. Furthermore, Chaplin (2013) suggested that lower frequency microwaves (915 MHz vs 2450 MHz) (MW) or radiofrequency radiation (RF) and even extremely low frequency fields (ELF) (3 Hz – 300 Hz) have significant and lasting effects on liquid water.

A number of studies regarding the application of electromagnetic radiation in the range of radiofrequencies and microwaves during freezing of food commodities have been recently published. Anese et al. (2012) carried out a study on the application of radio frequency radiation (RF) during freezing of meat. Although no data were presented on ice crystal size, the histological micrographs

seemed to indicate that the ice crystal size decreased under RF assisted freezing conditions. Hafezparast-Moadab et al. (2018) performed pulsed RF (27.12 MHz) assisted air blast freezing of fish. These results revealed that the RF assisted frozen fish had finer ice crystals (up to 75% smaller by surface), lesser damage to the structure, lower drip loss, and superior texture (close to fresh sample) than sample frozen in the absence of RF. Xanthakis et al. (2014) found smaller ice crystals and a decrease in the degree of supercooling under pulsed MW (2.45 GHz) assisted freezing. Moreover, they reported that freezing rate decreased when the power level of MW was increasing due to the heat generated by MWs. This study provided quantitative data regarding the ice crystal size and the impact of MW radiation during freezing of meat. The most recent study was on the application of MW assisted freezing of more sensitive structure food commodities such as fruits and vegetables (Jha et al., 2020), showing that MAF samples exhibited microstructure with smaller pores and more uniform size distributions compared to the control sample. The texture and the drip loss were also improved for MAF samples compared to the control sample. Jha et al., (2020), introduced also two concepts regarding the mechanism of action such as ”NITOM” concept (Nucleation Induced by Temperature Oscillation caused by MWs) and the ”NIMIW” (Nucleation Induced by constant or pulsed MIcroWaves power).

To explore this promising path, this work aims at characterising the effect of different MAF processing parameters on ice crystal formation. A Response Surface Method (RSM) has been used to correlate the combined effect of MW pulse width, power and the cooling rate on final crystal sizes, setting the basis for a better control of the crystallisation process.

2. MAIN SECTION

2.1. Material and methods

2.1.1. Sample preparation

Methylcellulose gel (Tylose) was chosen as model food in this work for its thermophysical and dielectric properties, which are close to those of meat products. Methylcellulose solutions (87% w/w water content) were prepared by stirring the mixture (water and methylcellulose) at ambient conditions for one hour. After pouring the mixture into plastic moulds, the samples were covered with aluminium foil to avoid evaporation and let in cold storage overnight for gelation. The size of the samples was 5.6 mm thick, 12 mm long and 8.3 mm wide.

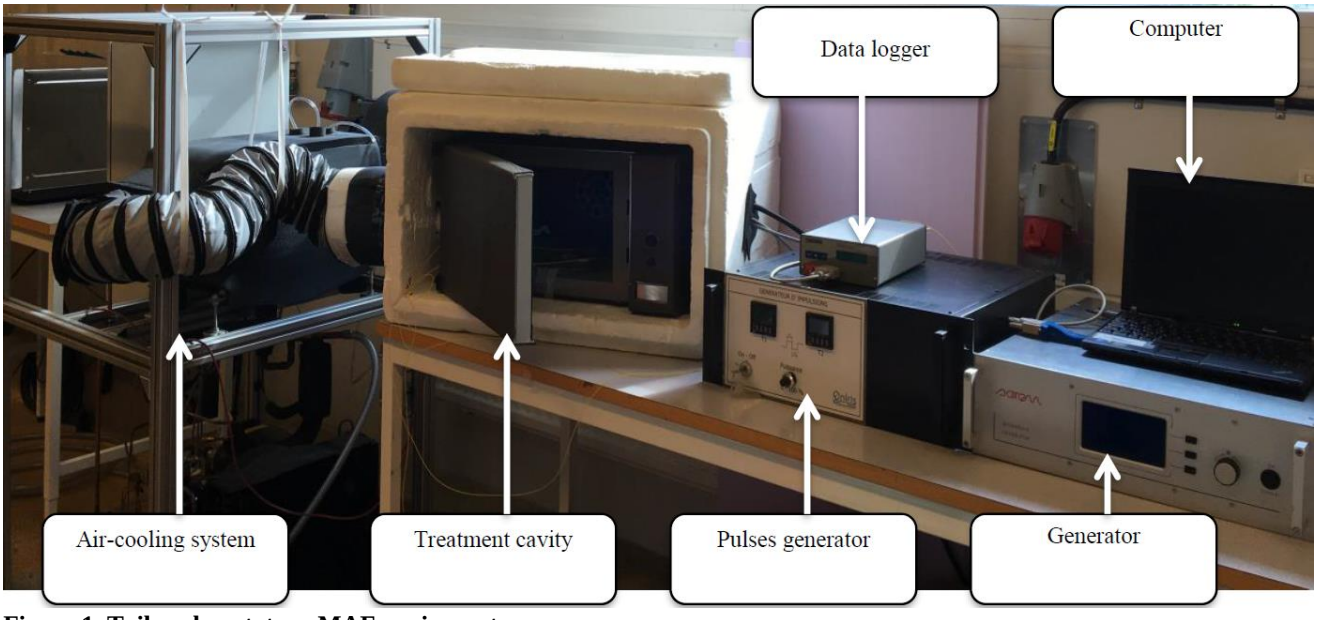

Figure 1. Tailored prototype MAF equipment

2.1.2. Microwave assisted – freezing equipment

A tailored experimental set up was used for the present work. This prototype equipment, shown in Fig. 1, consisted of a treatment cavity connected to a microwave solid-state generator (200W, SAIREM, NEYRON, France), which could emit constant power microwave radiation. The MW generator could be tuned to transmit pulsed electromagnetic radiation by a pulses generator connected to the analogic port. Freezing in the cavity occurred by means of an air-cooling circulating system, which was

connected by insulated hoses to a specially manufactured air inlet/outlet, which ensures high velocity air flow into the cavity without leakage of electromagnetic radiation. Moreover, optical fiber temperature sensors were used to record the temperature profile of the cavity (data logger, software Optilink).

2.1.3. Microstructure analyses

After freezing the samples under the different processing conditions, and freeze-dried in a benchtop freeze dryer (ALPHA 1–2 SDplus; Christ, Osterode am Harz, Germany). X-ray microtomography analysis (Skyscan1172 , Bruker, Germany) of the dried samples was carried out to measured crystal sizes for each sample. Before each set of scans, the rotation stage was aligned. Samples were scanned using 80 kV and 100 μA of source voltage and current, respectively, and were exposed during 300 ms per snap. The scans covered 180^{o} with a step of 0.4^{o}, 4 frames were averaged, and the resultant projected area was recorded for each rotation step. Due to the low density of the samples and the difference in X-ray absorption in comparison with the air absorption (in the voids), no filters were required for these scans. The voxel was a cube with an edge length of approximately 6 μm.

The projected images of each of the selected orientations were saved. With the use of a specialized algorithm, the distribution of X-ray attenuation in the volume can be reconstructed in order to obtain cross-sectional images. The final three-dimensional image was composed by piling the cross-sectional images, which look like if the object was sliced open along horizontal planes. In a standard two-dimensional image, the single picture elements are called pixels, however a microtomography cross-sectional image was composed of voxels (volume elements). This was due to the fact that they contained three-dimensional information including the width of the slice as well to the two-dimensional information of that specific slice.

Cross-sectional and three-dimensional images were reconstructed using NRecon software, where the ring effect and beam hardening were corrected. The misalignment was always kept between -10 and 10 voxels, as recommended for quantitative analysis.

The threshold is a crucial step for the pre-processing of the X-ray tomography images. As a result of the threshold, a binary image is obtained where the black pixels belong to the lower density phase (pores) whilst the white pixels belong to the compounds with the highest density (solids).

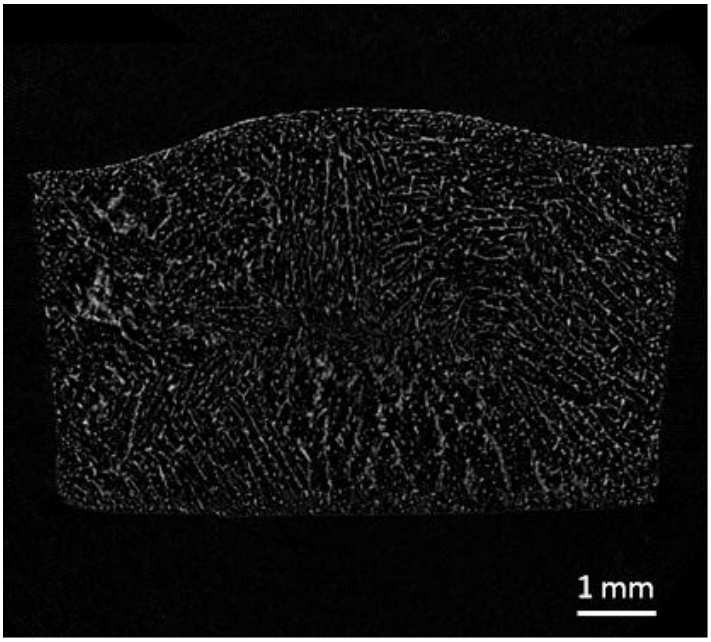

Figure 2. Representative X-ray microtomography cros-section scan micrographs of freeze dried samples after freezing.

2.1.4. Experimental design

Response Surface Method (RSM) (Hammami and Rene, 1997; Montgomery 2013) was employed to evaluate the effect of Pulses duration, Power levels and Cooling rates on crystal size of methyl cellulose MAF samples. Matlab software was used to design a CCD (Central Composite Design) for the three factors considered (i.e. independent variables Pulses, Power and Cooling rate) at five levels each (see Table 1).

This led to 17 experiments (including additional repetitions for the centre point), which are listed in Table 2.

The experimental data obtained for crystal size (D_{90} values presented in Table2) was then fitted to a full quadratic model of the following form:

$$y = \beta_0 + \sum_{i=1}^{n} \beta_i X_i + \sum_{i=1}^{n} \sum_{j=1}^{n} \beta_{ij} X_i X_j \qquad \text{Eq. (1)}$$

Table 1. Factors(coded and not coded) considered in Central Composite Design (CCD)

Factors	Levels				
	-1.68	-1	0	1	1.68
Pulses (s)	0	2	5	8	10
Power |(W)	0	2	5	8	10
Cooling rate (ºC/min)	0.16	0.5	1	1.5	1.84

where y is the fitted response (in this case fitted D_{90} value), β_0, β_i, β_{ij} are the regression coefficients and X_i, X_j are the independent variables or inputs. Statistical significance of each term in the model was evaluated using Analysis of variance (ANOVA) with 95% confidence level was performed for each response variable to test the model significance. The goodness-of- fit was determined using the lack-of-fit test and R^2 (coefficient of determination) and non-significant terms were excluded to avoid overfitting issues.

Table 2. Crystal size(μm) as given by the D_{90} index after microwave assisted freezing experiments performed according Central Composite Design (CCD).

Run	Pulses (s)	Power (W)	Cooling rate (ºC/min)	D_{90} (μm)
1	2	2	0.5	85.42 ± 20.71
2	2	2	1.5	72.58 ± 16.99
3	2	8	0.5	88.77 ± 18.81
4	2	8	1.5	75.07 ± 13.70
5	8	2	0.5	104.14 ± 21.17
6	8	2	1.5	65.28 ± 20.76
7	8	8	0.5	83.99 ± 9.91
8	8	8	1.5	71.62 ± 3.17
9	0	5	1	55.02 ± 8.29
10	10	5	1	60.82 ± 8.82
11	0	0	1	62.41 ± 7.19
12	5	10	1	70.85 ± 14.17
13	5	5	0.16	105.01 ± 4.66
14	5	5	1.84	68.21 ± 4.69
15	5	5	1	70.38 ± 13.92
16	5	5	1	55.70 ± 6.78
17	5	5	1	73.91 ± 6.15

2.2. Results

Fig.1 presents the measured D_{90} values (with standard deviations, error bars) for each one the experimental runs. The runs are sorted by crystal size from larger to smaller D_{90} values. Runs 13 and 5, the ones that produced larger crystals, correspond to slow cooling rates (0.16 and 0.5 ºC/min, respectively).On the other hand, the smaller sizes correspond to runs with cooling rates =1 ºC/min (run nos. 9, 10, 11) and power and pulses levels ranging on their extreme and center levels (see Table 2). These results suggest that the main factor determining crystal size is the cooling rate.

A quantitative description of the effect of the process variables (i.e. pulses, power and cooling rate) on the crystal size is given by the full quadratic model fitted to the available experimental data:

$$D_{90}^{fit,quad} = 119.80 + 6.76\,PS - 5.94\,PW - 88.65CR - 0.37PS * PW - 2.06PS * CR + 2.14PW * CR - 0.24PS^2 + 0.51PW^2 + 33.90CR^2 \qquad \text{Eq. (2)}$$

The comparison of experimental to fitted crystal sizes (i.e. D_{90} values), showed an overall good agreement between both data sets, with RMSE = 8.22 and R^2 = 0.86. However, the ANOVA analysis reveals lack of

significance (p =0.066>0.05), indicating the model is overfitted – this is, there are more terms/parameters than required to fit the data set. Attending to individual *p-values* for the regression coefficients, those corresponding to the quadratic terms for the pulses (PS^2) and power (PW^2), both with p-value >0.05 and thus non-significant, were removed. This led to a new reduced model in the form of a polynomial of first-order in *PS* and *PW* and second-order in *CR*. By regression analysis, the best fit to the experimental D_{90} values is given by:

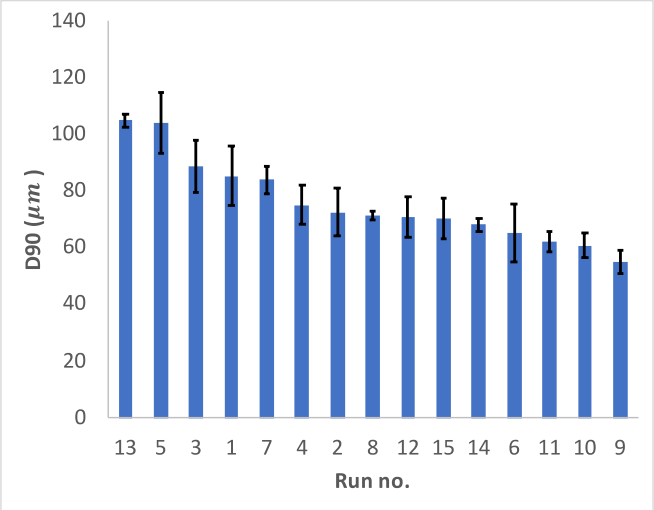

Figure 1. Experimental runs conducted for the microwave assisted freezing of tylose sorted by resulting crystal sizes, from larger to smaller. Crystal size is defined by the D_{90} index. All runs were triplicated – black bars show the corresponding standard deviations. The graph does not include the centre point repetitions. (Runs no. 16 and 17).

$$D_{90}^{fit,poly} = 116.66 + 3.54\,PS - 1.09\,PW - 89.33CR - 0.24PS * PW - 2.06PS * CR + 2.13PW * CR + 34.24CR^2 \quad \text{Eq. (3)}$$

with RMSE = 9.13 R^2 = 0.78 and p=0.012 for the model. D_{90} values fitted using Eq. (3) are compared in Figure 3 to the experimental ones, showing the goodness of fit of the polynomial model - most of the fitted points lay within the experimental error for their corresponding conditions.

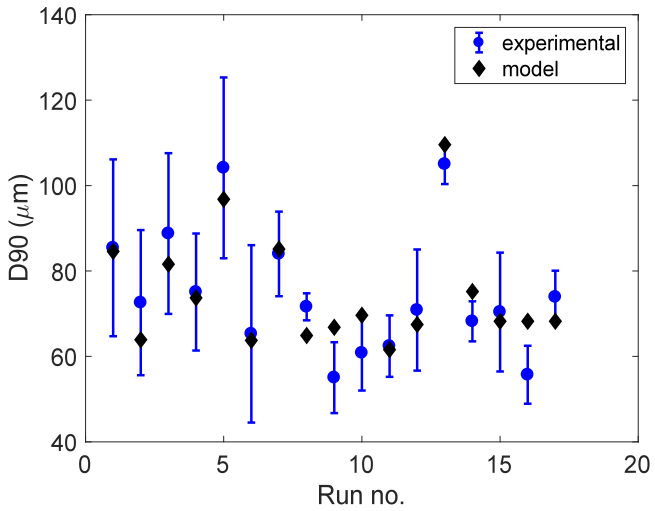

Figure 3. Fitted (black diamonds) using a second order model for the cooling rate and first order for the other two factors (i.e. pulses and power), including interactions vs. measured crystal sizes (blue dots) as given by the D90 index for the microwave assisted freezing of tylose. This model is significant (p=0.016<0.05) and includes all the factors.

Finally, interaction effects between factors in the polynomial model are illustrated in Figure 5. The interaction between the cooling rate (critical factor) and the pulses duration is presented in Fig. 5(i) for PW = 0 W (ii) PW = 5 W and (iii) PW = 10 W. These set of contour plots reveal that smaller crystals (i.e. D_{90} values) are obtained with pulses durations within 6 and 8 seconds. This region shifts from slow cooling rates (0-0.5 ^{o}C/min) to

mid/fast ones (1-1.5 ºC/min) as the power increases (see Fig. 5(i), (ii) (iii)). These three graphs also indicate that, for each power level, larger crystals sizes are consistently obtained by a combination of fast cooling rates and short pulses.

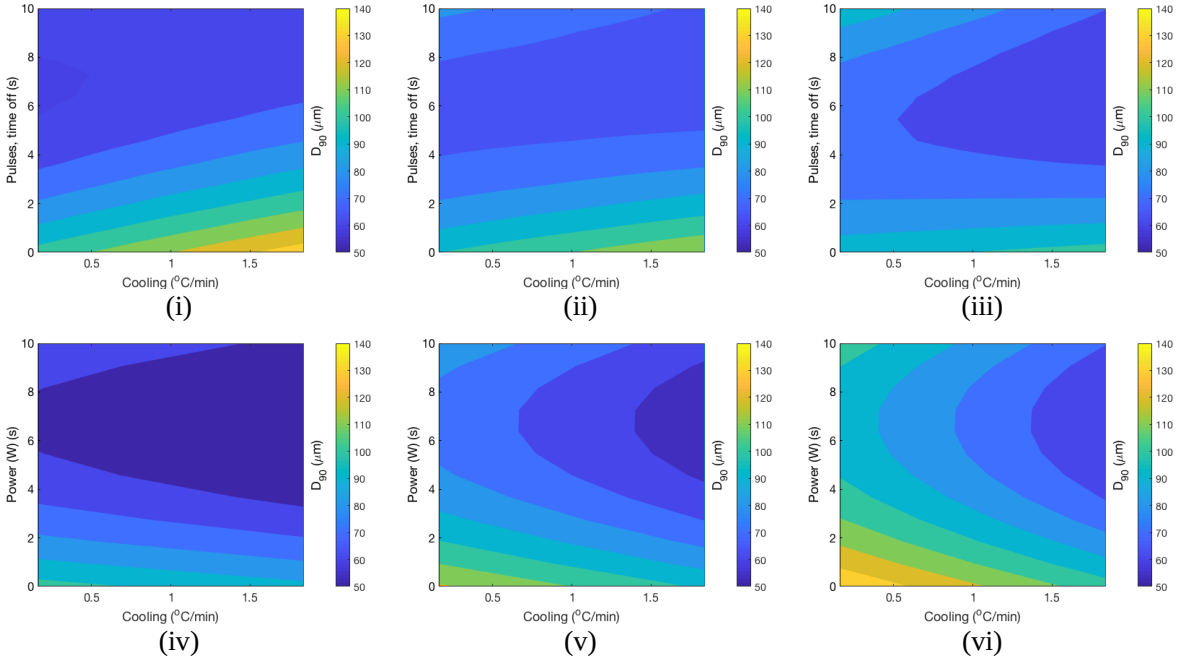

Figure 5. Response surface graphs for crystal size (D_{90}) as given by the fitted polynomial model (a) Interaction of Cooling rate and Pulses, with Power fixed at its center level (Power = 5 W) (b) Interaction of Cooling rate and Power, with Pulses at its center level (Pulses = 5 s off).

Fig. 5 (iv), (v) and (iv) represent the interaction between cooling rates and power levels for PS = 0 s (i.e. no pulses), PS = 5s and PS = 10s, respectively. The region of smaller D_{90} values (dark blue area) seats within intermediate power levels, within approximately 6 W and 8 W, and it also shifts towards regions defined by fast cooling rates as the pulses duration increases – it extended across all cooling rates in Fig.5(iv) to then moved to CR > 1.5ºC/min in Fig. 5(vi). For this case, the combination of slow cooling rates and lower power levels produced the larger crystal sizes (yellowish areas at the bottom left).

Those results can explain previous studies on microwave assisted food freezing where both pulsed and constant microwave irradiation during freezing have shown the ability to produce smaller as well as greater ice crystal under specific conditions (Xanthakis et al., 2014), (Xanthakis et al., 2018) and (Jha et al., 2020). It can be mentioned that there are critical zones of the three factors (MW power level, pulse width and cooling rate) combinations which can be used to achieve a desired size of ice crystals. The two proposed concepts by Jha et al., (2020) regarding the mechanism of action such as ”NITOM” concept (Nucleation Induced by Temperature Oscillation caused by MWs) and the ”NIMIW” (Nucleation Induced by constant or pulsed MIcroWaves power) seemed to be valid under specific freezing parameter combinations. More specifically, NITOM” concept was based on the fact that under specific duty ratio, the temperature of the sample undergoing freezing will oscillate and favour secondary nucleation which in turn will suppress the crystal growth. The second, NIMIW concept was based on constant or pulsed (short time) emission. MW radiation will influence the hydrogen bonds between water molecules, which may affect the water cluster structures during freezing. According the authors, it is expected that MWs would exert a torque and displace the water molecules from their equilibrium relationships in the ice cluster resulting in fragmentation of existing ice crystals when the crystals are in the form of nuclei. Those fragmented ice crystals nuclei may act as new nucleation sites and promote the secondary nucleation, thus, causing ice crystal size reduction (Jha et al., 2020).

3. CONCLUSIONS

This work investigated the effect of process conditions on the ice crystal size resulting from microwave assisted freezing (MAF) processes. Samples of methyl cellulose food model system were processed following an experimental design that combined 5 different levels for the most relevant factors (i.e. pulses duration, power amplitude and cooling rates) and analysed using micro-CT to measure characteristic crystal sizes. The obtained D_{90} values were then fitted to quadratic models following a response surface methodology (RSM). Results revealed that the cooling rate was the critical factor controlling D_{90} at the studied

conditions. A polynomial model – first-order for the pulses and power factors and second-order for cooling – was able to reproduce accurately the experimental data set. Interaction effects derived from the surface response model revealed that mid levels (within the range here studied) of both pulses and power amplitudes resulted in the smallest crystal sizes (ca. 50-60 μm) for cooling rates > 1.5 ^{o}C/min. Overall, this work shows that modelling approaches, like RSM, can be used to define a theoretical map for processing conditions during MAF processes that correlates, and potentially predicts, resulting crystal sizes. This study can be useful for the control of ice crystal size during microwave assisted freezing processes.

ACKNOWLEDGEMENTS

Authors Patricia Andreu-Cabedo and Estefania Lopez-Quiroga thank financial support received from EPSRC (grant no. EP/S023070/1). Graziele Gustinelli and Epameinondas Xanthakis received funding from the Swedish Research Council FORMAS, under the FREEZEWAVE project (SUSFOOD – ERANET, SE: 2014-1925).

REFERENCES

Anese, M., Manzocco, L., Panozzo, A., Beraldo, P., Foschia, M., & Nicoli, M. C., 2012. Effect of radiofrequency assisted freezing on meat microstructure and quality. *Food Res. Int.* 46(1), 50–54.

Chaplin, M., 2013. http://www1.lsbu.ac.uk/water/

Dalvi-Isfahan, M., Hamdami, N., Le-Bail, A., Xanthakis, E., 2016. The principles of high voltage electric field and its application in food processing: a review. *Food Res. Int.* 89 (1), 48–62.

Dalvi-Isfahan, M., Hamdami, N., Xanthakis, E., Le-Bail, A., 2017. Review on the control of ice nucleation by ultrasound waves, electric and magnetic fields. *J. Food Eng.* 195, 222–234.

Hafezparast-Moadab, N., Hamdami, N., Dalvi-Isfahan, M., & Farahnaky, A., 2018. Effects of radiofrequency-assisted freezing on microstructure and quality of rainbow trout (Oncorhynchus mykiss) fillet. *Innov. Food Sci. Emerg.* 47, 81-87.

Hammami, C., René, F.,1997. Determination of freeze-drying process variables for strawberries. *J. Food Eng.* 32 (2), 133-154.

Jha, P. K., Xanthakis, E., Jury, V., Le-Bail, A., 2017. An Overview on Magnetic Field and Electric Field Interactions with Ice Crystallisation; Application in the Case of Frozen Food. *Crystals* 7, 299.

Jha, P. K., Sadot, M., Vino, S. A., Jury, V., Curet, S., Rouaud, O., Havet, M., Le-Bail, A., 2017. A review on effect of DC voltage on crystallization process in food systems. *Innov. Food Sci. Emerg.* 42, 204 – 209.

Jha, P.K., Chevallier, S., Xanthakis, E., Jury, V., Le-Bail, A., 2020. Effect of innovative microwave assisted freezing (MAF) on the quality attributes of apples and potatoes. *Food Chem.* 309, art. no. 125594.

Le-Bail, A., Jha, P., Xanthakis, E., Havet, M., Jury, V., 2016. Phase change under static electrical field; in the case of lipids. *Refrigeration Science and Technology* 2016, 138-143.

Montgomery, D.C., 2013. Design and analysis of experiments, 8th Edition. John Wiley and Sons. Hoboken, NJ, USA.

Sadot, M., Curet, S., Rouaud, O., Le-Bail, A., Havet, M., 2017. Numerical modelling of an innovative microwave assisted freezing process. *Int. J. Refrig.* 80, 66-76.

Xanthakis, E., Havet, M., Chevallier, S., Abadie, J., Le-Bail, A., 2013. Effect of static electric field on ice crystal size reduction during freezing of pork meat. *Innov. Food Sci. Emerg.* 20*, 115–120.*

Xanthakis, E., Le-Bail, A., Ramaswamy, H., 2014. Development of an innovative microwave assisted food freezing process. *Innov. Food Sci. Emerg.* 26, 176–181.

Xanthakis, E., Huen, J., Eliasson, L., Jha, P.K., Le-Bail, A., Shrestha, M., 2018**.** Evaluation of microwave assisted freezing (MAF) impact on meat and fish matrices. *Refrigeration Science and Technology* 2018, 176-181.